



HAL
open science

Optimum and Rapid Annealing of Nanocrystalline $\text{Fe}_{73.5}\text{Cu}_1\text{Nb}_3\text{Si}_x\text{B}(22.5-x)$ Ferromagnets-Correlation Between Magnetic, Mechanic and Thermal Analysis

F. Mazaleyrat, B. Tirollois, P. Lepeut, J. Rialland

► **To cite this version:**

F. Mazaleyrat, B. Tirollois, P. Lepeut, J. Rialland. Optimum and Rapid Annealing of Nanocrystalline $\text{Fe}_{73.5}\text{Cu}_1\text{Nb}_3\text{Si}_x\text{B}(22.5-x)$ Ferromagnets-Correlation Between Magnetic, Mechanic and Thermal Analysis. *Journal de Physique III*, 1996, 6 (2), pp.217-224. 10.1051/jp3:1996119 . jpa-00249451

HAL Id: jpa-00249451

<https://hal.science/jpa-00249451>

Submitted on 4 Feb 2008

HAL is a multi-disciplinary open access archive for the deposit and dissemination of scientific research documents, whether they are published or not. The documents may come from teaching and research institutions in France or abroad, or from public or private research centers.

L'archive ouverte pluridisciplinaire **HAL**, est destinée au dépôt et à la diffusion de documents scientifiques de niveau recherche, publiés ou non, émanant des établissements d'enseignement et de recherche français ou étrangers, des laboratoires publics ou privés.

Optimum and Rapid Annealing of Nanocrystalline $\text{Fe}_{73.5}\text{Cu}_1\text{Nb}_3\text{Si}_x\text{B}_{(22.5-x)}$ Ferromagnets—Correlation Between Magnetic, Mechanic and Thermal Analysis

F. Mazaleyrat (^{1,*}), B. Tirollois (¹), P. Lepeut (²) and J. F. Rialland (¹)

(¹) Laboratoire d'Électricité, Signaux, Robotique, E.N.S. de Cachan,
61 avenue du président Wilson, 94235 Cachan Cedex, France

(²) Laboratoire Matériaux Minéraux, Conservatoire National des Arts et Métiers,
292 rue Saint Martin, 75141 Paris Cedex 03, France

(Received 12 June 1995, revised 7 November 1995, accepted 16 November 1995)

PACS.64.70.Pf – Glass transitions

PACS.75.50.Kj – Amorphous magnetic materials

PACS.75.60.Nt – Magnetic annealing and temperature-hysteresis effects

Abstract. — In this paper we discuss the optimal and rapid treatment of $\text{Fe}_{73.5}\text{Cu}_1\text{Nb}_3\text{Si}_x\text{B}_{22.5-x}$ nanocrystalline alloy. In order to define an optimisation parameter of the coupled temperature/annealing time, several treatments of two alloys ($x = 13.5\%$ and $x = 15.5\%$) have been studied. A rapid annealing (630 °C with no step) which gives rise to better magnetic properties is proposed. It is shown that the alloy containing 15.5% of silicon is mechanically stronger when rapidly treated. Finally, it is attempted to correlate magnetic, mechanical and thermal analysis showing also how this can help to gain insight into magneto-mechanical coupling through amorphous and crystalline phase.

Résumé. — Dans ce travail on étudie les traitements thermiques optimaux et rapides de l'alliage $\text{Fe}_{73.5}\text{Cu}_1\text{Nb}_3\text{Si}_x\text{B}_{22.5-x}$ nanocristallin. Nous avons essayé différents traitements avec deux alliages ($x = 13,5\%$ et $x = 15,5\%$) et nous avons défini un paramètre d'optimisation du couple température/durée de recuit. Nous proposons un recuit rapide (630 °C sans palier) qui permet d'améliorer les performances magnétiques et nous montrons aussi que l'alliage contenant 15,5 % de silicium est mécaniquement plus résistant quand il est recuit de cette manière. Enfin, nous essaierons de corrélérer les analyses magnétiques, mécaniques et thermiques.

1. Introduction

Evidence of existence of couples temperature/annealing time (T/t) have been shown by several authors [1, 2] observing alike X-ray diffraction figures for different temperatures (T) and different step duration (t). They inferred from those works that various T/t combinations could generate crystallization stage of similar compounds, but this results in different effects on magnetic quantities. This could be partly explained by a different grain size distribution and partly by a different state of internal stresses. In fact, crystallization causes a local

(*) Author for correspondence (e-mail: Frederic.Mazaleyrat@lesir.ens-cachan.fr)

Table I. — *Annealing conditions and denotations of samples.*

temp. (K)	time (min)	$x = 15.5\%$	$x = 13.5\%$
as-cas	-	AC	BC
823	30	A1	B1
853	60	A2	B2
873	60	A3	B3
903	60	A4	B4
823	30	A5	B5
903	3	A6	B6
903	0	A7	B7
791	60	-	B8

decrease of volume, and produces stress between the two phases. Then, these internal stresses depend on the crystallization kinetics through amorphous relaxation, thereby, on the couple temperature/annealing time. As Young's modulus of amorphous phase is different from crystal one (≈ 150 MPa for most of metallic glasses, > 220 MPa for crystalline FeSi), external strain generates high internal stresses that explains cleavage fracture. So, it is certain that by increasing fractional volume of crystalline phase, brittleness is raised. However, this is not compatible with a high quality of magnetism because crystalline fraction must be about 60% to exhibit good magnetic properties [3]. In other respects, it could be interesting for industrial production to reduce annealing time with a view to minimize energy and time of production. Hence the aim of this paper is to find optima by taking into account of all these problems.

2. Experimental Details

2.1. ANNEALING. — All samples are annealed under Argon atmosphere. The treatment furnace was specially designed to have a highly uniform temperature along the samples. Many annealing time/temperature (T/t) combinations are investigated on flat ribbons for two different alloys which are annealed according to temperature cycles, as listed in Table I. Heating rate was 10 K/min and cooling rate was 10 K/min, until natural cooling (above 550 K).

2.2. MAGNETIC TESTING. — As these materials are meant for medium frequency purposes, they are tested under controlled sinusoidal flux in the frequency range from 1 to 100 kHz. A single sheet tester with ferrite double yoke is used. Losses in the yokes are evaluated by measurements and are found to be less than 10^{-4} J/m³ at 100 kHz for 1.2 T induction in the ribbon. Henceforward, these losses will be neglected. The flux is detected by ultra fine winding coil and computed after air-flux compensation. The magnetic field is calculated from excitation current. Electromagnetic losses are determined by calculation of the hysteresis loop area.

2.3. THERMAL ANALYSIS. — The crystallization kinetics are investigated by Differential Thermal Analysis (D.T.A.) from 300 to 1200 K with a heating rate of 40 K/min for annealed samples and 40, 20, and 10 K/min for as-cast samples. These analysis are run with stainless steel and alumina references. Results are plotted after normalization to the sample mass.

2.4. MECHANICAL TESTING. — This test evaluates the Young's modulus and the fracture strength of as-cast and annealed ribbons. The samples are 50 mm long, 9 or 10 mm wide and 20 or 17 μ m thick respectively.

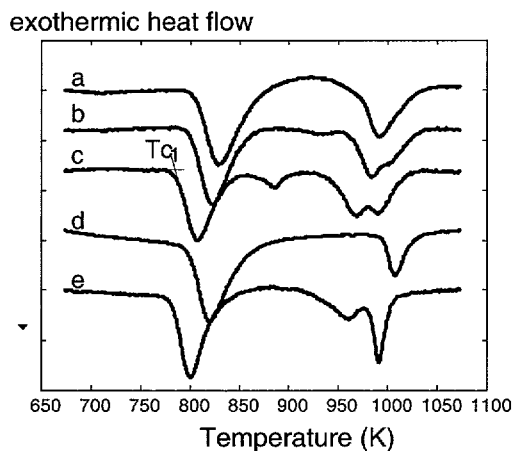


Fig. 1. — ATD plots obtained during continuous heating at rate of 40 (a), 20 (b) and 10 K/min (c) on as cast B sample, 40 (d) and 10 K/min (e) on as cast A sample.

A pneumatic uniaxial traction device is used, configured for a 5 kN maximum strength—corresponding to a 27.7 GPa maximum stress for $180 \times 10^{-9} \text{ m}^2$ section. The tensile force measurement accuracy is 1 N, which gives, in our case, about 5.5 MPa accuracy. The displacement is gauged by optical tracking of two reflection targets, the maximum resolution is $5 \mu\text{m}$ and the rate of stressing is 0.1 mm/min.

3. Experimental Results

Many papers have been published about optimum annealing. They show that the best temperature of treatment is located between 823 K (550 °C) and 853 K (580 °C) and its duration is one hour [4,5]. In the aim of minimizing energy and time of manufacturing, an attempt was made to reduce the step duration as much as possible and it was clear that only increasing the temperature could allow it. In order to represent, on the same plot, quantities issued from various T/t combinations, we search for a self consistent rule of thumb as a function of temperature and time.

It is obvious that temperature depends on the reference (absolute or Celsius zero, room temperature...). So, in order to be significant, we have to use a firm reference temperature inherent to the material and related to crystallization kinetics. Here it is thought that the temperature of crystallization (T_{C1}) is the most characteristic one because it is the first and the only granulation stage during annealing. This temperature is defined from DTA plots obtained with the same heating rate as treatment (Fig. 1, curve C). It is found that T_{C1} is 778 K for $x = 15.5$ and 783 K for $x = 13.5$.

After several attempts this parameter was defined by the following:

$$\Theta = \int (T - T_{C1}) dt \quad [\text{K s}]$$

where Θ represents the area of the temperature cycle above T_{C1} .

As illustrated by graphic in Figure 2, this representation of losses (1 kHz, 0.8 T) vs. Θ is coherent. Even though we observe a small dispersion, this may be interesting if we consider it

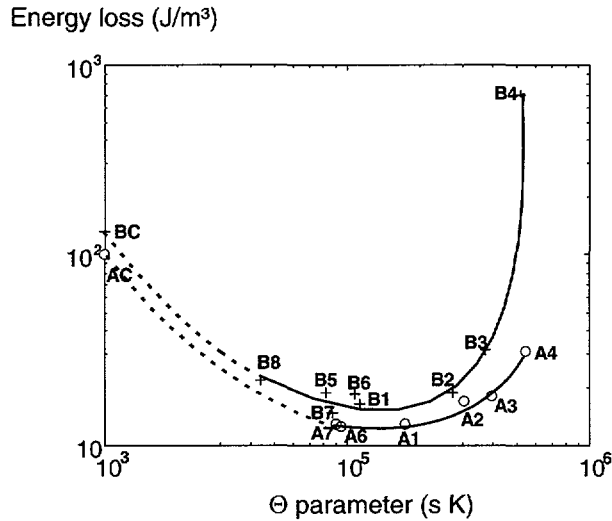


Fig. 2. — Electromagnetic losses at 1 kHz, 0.8 T as function of Θ parameter (\circ) \rightarrow A alloy, (+) \rightarrow B alloy.

just as a convenient representation. The lowest losses have been obtained for various combinations of temperature and step duration, i.e. Θ varying from 4.5×10^4 to 2×10^5 s K (minimum about 10^5 s K).

Maximum permeability at 1 kHz is 51 000 and 38 000 for A and B ribbon respectively, which are treated at 823 K (550 °C) for 60 min. This maximum reaches 57 000 with rapid annealing, which is 12% and 50% above. We note that, even though magnetic properties are not significantly different between A6 and A7, permeability strongly decreases for 923 K (630 °C) annealing of B ribbon, if the step duration is increased from 0 to 3 minutes.

With rapid heating, initial permeability (1 kHz, 50 mT) grows up to 28 000, for $x = 15.5$, and 19 000, for $x = 13.5$, while it is about 17 000 for both of them with classic annealing.

Losses are presented vs. induction at 10 kHz in Figure 3 (we show here only the most useful results for the following analysis). The advantage of rapid heating is evident. At high induction, losses are lower than in every treatment we made and also lower than values generally found in literature (we have found 26 J/m^3 at 1 T, 1 kHz; 80 J/m^3 at 1 T, 100 kHz, for $x = 15.5\%$).

In Figure 3, we can also observe a rise in losses for B6 compared to B7, while losses for A6 (not represented) are strictly equal to A7. This is relative to permeability falling (see above) and it is strongly correlated with greater increase of losses for B4 and B3 compared to A4 and A3 (Fig. 2).

We have performed thermal analysis on as-cast and annealed ribbons. For annealed ribbons, we must carry out DTA at high heating rate (40 K/min), because the analysis must not induce new crystal growth. For as-cast ribbons, the heating rates are 40 K/min, in order to compare results with results from annealed ribbons and 10 K/min, to have crystallization kinetics similar to that of the annealing during temperature rise. We also made 20 K/min analysis to confirm the evolution of peaks with respect to heating rate.

As is shown in Figure 1, for 13.5% silicon content, at 40 K/min (Curve a), the first exotherm is located at a 828 K peak temperature. According to previous works, it represents αFe crystallization [6], and the second peak (993 K), corresponds to FeB crystallization. For 20 K/min

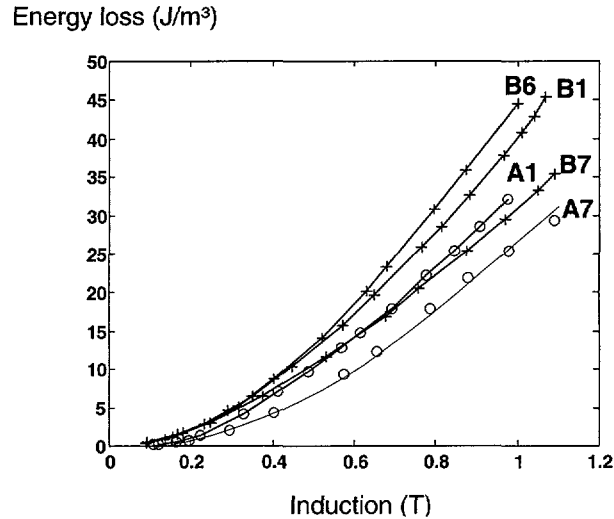


Fig. 3. — Total losses at 10 kHz vs. induction for classical and rapid annealing (○)→ A alloy, (+)→ B alloy.

DTA plot (Curve b), the first exotherm is shifted at 823 K and the second, at about 983 K, shows an important shoulder close to 1000 K. As can be seen on 10 K/min DTA plot (Curve c), a third crystallization stage, overlapped by the second, clearly appears at 990 K. This was suspected by different authors [4,7,8] and we suggest that two different compound formations take place in this range. In contrast, the exotherm revealed at about 885 K appears not to have been observed before. This has been confirmed with several samples and two distinct inert references (stainless steel and alumina). For 15.5% silicon content, two peaks are shown in Curve d at 820 K and 1005 K with a 40 K/min heating rate. In Curve e (10 K/min), the first peak is located at 800 K and the second separates with a peak at 960 K and an other at 990 K. It is remarkable that the last exotherm is located at a temperature of 990 K for the two alloys (Curves c and e): this may indicate nucleation of similar compounds.

DTA plots of annealed ribbons are identical in appearance for 823 K/1h, 903 K/0 and 903 K/3 min annealing and give no significant results as the peaks were proved to be equal in area, except for B6 for which a smaller area may be due to crystallization which corresponds to the 985 K peak observed on B as-cast tape.

To improve mechanical properties, micro hardness measurements with as-quenched and annealed ribbons were first tried, but the hardness scattering was too large to offer evidence of variations as a function of annealing conditions. However, Vickers hardness was found to be 950 kg/mm² for as-cast tapes and various values between 1200 and 1500 kg/mm² for annealed ones, with an average value of 1380. It is noted that these results are not in good agreement with Varga *et al.* [7], but in all cases hardness is increased by annealing.

We also have tested strength properties in order to evaluate Young's modulus and ultimate strength. As it was attempted, we observe cleavage fracture for all ribbons with no plastic flow as found for all glassy solids. In Table II, we present average values from tests made on several samples treated under the same conditions. This table shows that the Young's modulus of B alloy is slightly higher for rapid annealing while it's more brittle. By opposition, for rapid annealing of A ribbon, elastic modulus is slightly lower while fracture strength increases.

Table II. — *Young's modulus and fracture stress for several treatments of A and B alloys. $\Delta E/E$ is the variation of Young's modulus with respect to as-cast one and $\Delta\sigma_r/\sigma_r$ is the variation of ultimate strength with respect to as-cast one.*

Si contents	annealing	E (Young's modulus)	$\Delta E/E$	σ_r (breakage strength)	$\Delta\sigma_r/\sigma_r$
13.5%	BC as-cast	135 GPa		974 MPa	
	B1 823 K/1h	177 GPa	+31%	822 MPa	-15%
	B7 903 K	180 GPa	+33%	566 MPa	-42%
15.5%	AC a-cast	162 GPa		2405 MPa	
	A1 823 K/1h	187 GPa	+15%	745 MPa	-69%
	A7 903 K	182 GPa	+12%	1128 MPa	-53%

4. Discussion

These experiments show clearly the advantages of rapid annealing. Firstly, total annealing time is reduced from 3 to 2 hours, representing a cost-performance trade-off improvement. Secondly, even if low induction losses ($B < 0.3$ T) are equal for rapid and classical annealing, high induction losses are lower (-20% at 10 kHz, 1 T). As nanocrystalline materials, compared to cobalt based amorphous, are to be used at high induction, it is obvious that we have to compare losses for induction about 1 T and not 0.2 T as usually done. The effect of rapid annealing on A strip is better than on B. In order to explain that, we have performed 903 K annealing with 3 min and one hour steps. As we said, there is no difference between A6 and A7 while B6 properties deteriorates compared to B7. We also showed that A4 degradation is weaker than B4 (Fig. 2). This is reasonably attributable to the crystallization stage detected at 885 K with B ribbon (Fig. 1). However, we do not have enough matter and more work has to be done in this area, e.g. X-ray diffraction has to be performed to determinate the nature of this crystallization.

In the other hand, it was seen that A7 breakage strength is much higher than A6, and that it is strictly the opposite for B7 and B6. If we evaluate ultimate strength as relative values with respect to as-cast quantities, we observe greater variation for the A alloy (Tab. II). This is probably due to a greater interface area because, in the same annealing conditions, the part of crystallized volume is always greater for higher silicon contents [3]. In each case, it is clear that fracture strength is lower for the treatment which gives the greater Young's modulus. This tendency is a well known result in metallurgy: annealing of amorphous results in drop of fracture strain and increase of elastic modulus and hardness [9] and crystallization makes Young's modulus increase.

The fact that the structure of the nanocrystalline material becomes heterogeneous, clearly make the ribbon more brittle. We can explain this phenomenon qualitatively in Figure 4. As amorphous phase elastic modulus (E_a) is lower than one of crystals (E_c), it is obvious that amorphous suffers a greater strain, so this makes the material more brittle as the crystallized part increases. It follows that fracture strength is lower. This could be confirmed if we assume that mechanical properties of amorphous phase are like that of as-quench properties, but this should be taken with some degree of reservation because annealing causes the composition of amorphous to change. It is also possible that the structure becomes loose at the interface between amorphous phase and grains, as the interface must be Niobium rich [10].

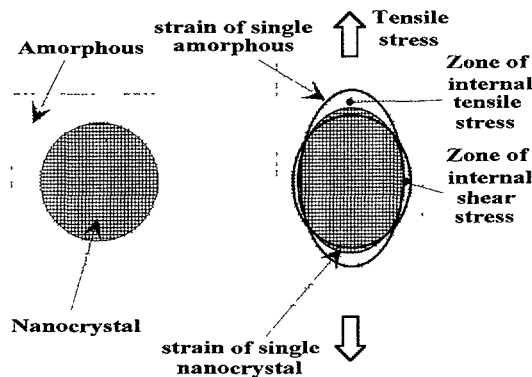


Fig. 4. — Origin of internal stresses induced by external tensile stress.

Loss evaluation suggests that rapid heating optimizes magnetic structure. It is expected that this treatment gives rise to a lower state of internal stresses. Mechanical testing of A alloy could confirm it as rupture strength is greater for A6.

5. Conclusion

Finally, we conclude that, from a magnetic point of view, rapid annealing gives the best results. Nevertheless, in the case of B alloy ($x = 13.5\%$), because the brittleness is higher for rapid annealing, the choice between rapid and classical treatments is an open question. Further criterion, such as quick ageing, could help in answering to this question and need, now, to be investigated. The existence of a crystallization peak located at 885 K, could be responsible for magnetic instability against ageing, especially with rapidly annealed ribbons.

In the case of A alloy ($x = 15.5\%$), from several points of view, it is certain that rapid heating results in better properties. Hence, it seems that rapidly heated $\text{Fe}_{73.5}\text{Cu}_1\text{Nb}_3\text{Si}_{15.5}\text{B}_7$ is likely to give the best performances in terms of losses, permeability and brittleness.

References

- [1] Yoshizawa Y. and Yamauchi K., Change of magnetic properties with annealing conditions in FeCuNbSiB alloy, *J. Jpn Metals* **55** (1991) 589-595.
- [2] Müller M., Mattern N. and Illgen L., The influence of the Si/B content on the micro structure and the magnetic properties of soft nanocrystalline alloys, *Z. Metallkde* **82** (1991) 895-901.
- [3] Ueda Y., Ikeda S. and Minami K., Precipitation of α -Fe and structure for amorphous FeCuNbSiB alloys by annealing, *Mat. Sc. & Engineering A* **181/182** (1994) 992-996.
- [4] Bigot J., Lecaude N., Perron J.C., Milan C., Ramiarinjaona C. and Riolland J.F., Influence of annealing conditions on nanocrystallization magnetic properties in FeCuNbSiB, *J.M.M.M.* **133** (1994) 299-302.

- [5] Herzer G., Magnetization process in nanocrystalline ferromagnets, *Mat. Sc. & Engineering A* **133** (1991) 1-5.
- [6] Varga L.K., Kisdi-Koszo E., Zsoldos E. and Bakos E., Optimisation of the heat treatment for the nanocrystalline FeCuNbSiB alloys, *IEEE Trans. Mag.* **30** (1994) 522-554.
- [7] Varga L.K., Bakos E., Kiss L.F. and Bakonyi, The kinetics of amorphous-nanocrystalline transformation for a Finemet alloy, *Mat. Sc. & Engineering A* **179/180** (1994) 567-571.
- [8] Conde C.F. and Conde A., Amorphous to nanocrystalline transformation of a Finemet-type alloy, Proc. ISMANAM-94, *Mat. Sci. Forum* **179-881** (1995) 581.
- [9] Luborsky F.E., Amorphous metallic alloys (Butterworths, Sevenoaks, Kent, U.K., 1983) pp. 204-225.
- [10] Yavari A.R. and Drhohlav O., *Mater. Trans. JIM* **36** (1995) 896.